5
MULTI-SCALE MODELING PROGRAMME

The group was established in 2011 as an emerging, effective and future-oriented modeling program fully exploiting the power of HPC at CSIR-4PI, initially in the field of atmospheric sciences to advance the simulation of weather and climate, to project future climate change, assess associated vulnerability and provide efficient adaptation and mitigation strategies. Moreover, this is a data intensive paradigm where numeric's and computing strategies relevant for different scales in a dynamical system are combined to arrive at an effective computational solution than the one obtained from the strategy dealing with the most relevant single scale. In initial phase of the program, the group sought to develop an ultra-high resolution weather and climate model framework to address multi-scale processes of the atmosphere and analyze the data from observations and these simulations to effectively arrive at inferences. General Circulation Models (GCMs), coupled ocean-atmosphere climate model and earth system model with emphasis on processes such as multi scale organization of organized convection and aerosol-cloud-radiation feedbacks, were employed.

Inside

5.1 Prediction of Indian rainfall during the summer monsoon season on the basis of links with equatorial Pacific and Indian Ocean climate indices

Our study attempts to develop simple empirical models for prediction of all-India rainfall (AIR) during the summer monsoon season (Indian Summer Monsoon Rainfall or ISMR), based on a composite index of El Niño Southern Oscillation (ENSO) and Equatorial Indian Ocean Oscillation (EQUINOO).The following data sets for the period 1958-2010, were used in this study: (i) ISMR and updates from Indian Institute of Tropical Meteorology (http://www.tropmet.res.in), (ii) NINO3.4 index [sea surface temperature (SST) anomaly over NINO3.4 (120°–170°W, 5°S–5°N) region] obtained from Climate Analysis Section, National Center for Atmospheric Research, USA (http://www.cgd.ucar.edu), (iii) surface wind data from National Center for Environmental Prediction (http://www.cdc.noaa.gov) and (iv) DMI, the Indian Ocean Dipole mode index from http://www.jamstec.go.jp.

The ENSO index is defined as the negative of the NINO3.4 SST anomaly (normalized by the standard deviation). We use an index of EQUINOO based on the anomaly of the zonal component of the surface wind at the equator (60°E–90°E, 2.5°S–2.5°N). The zonal wind index (henceforth EQWIN) is taken as the negative of the anomaly of the zonal wind so that positive values of EQWIN are favourable for the monsoon.

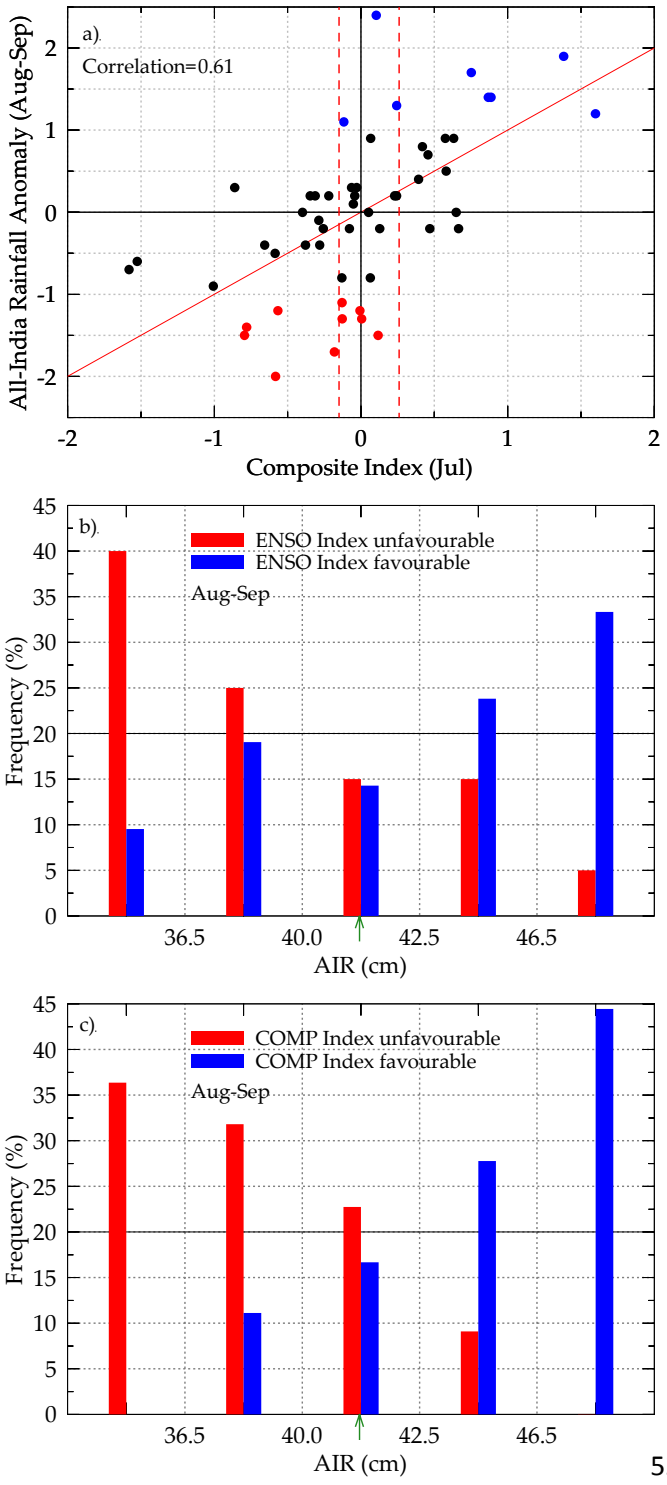

Figure 5.1 a) Normalized all India rainfall anomaly predicted for August-September rainfall against the composite index for July (a); Frequency of occurrence (%) in different categories of normalized August-September anomalies for years for favourable & unfavourable values of ENSO index (b); and of the composite index (c). Green arrows in the x-axes in (b) and (c) indicate climatological mean August-September all-India rainfall (AIR).

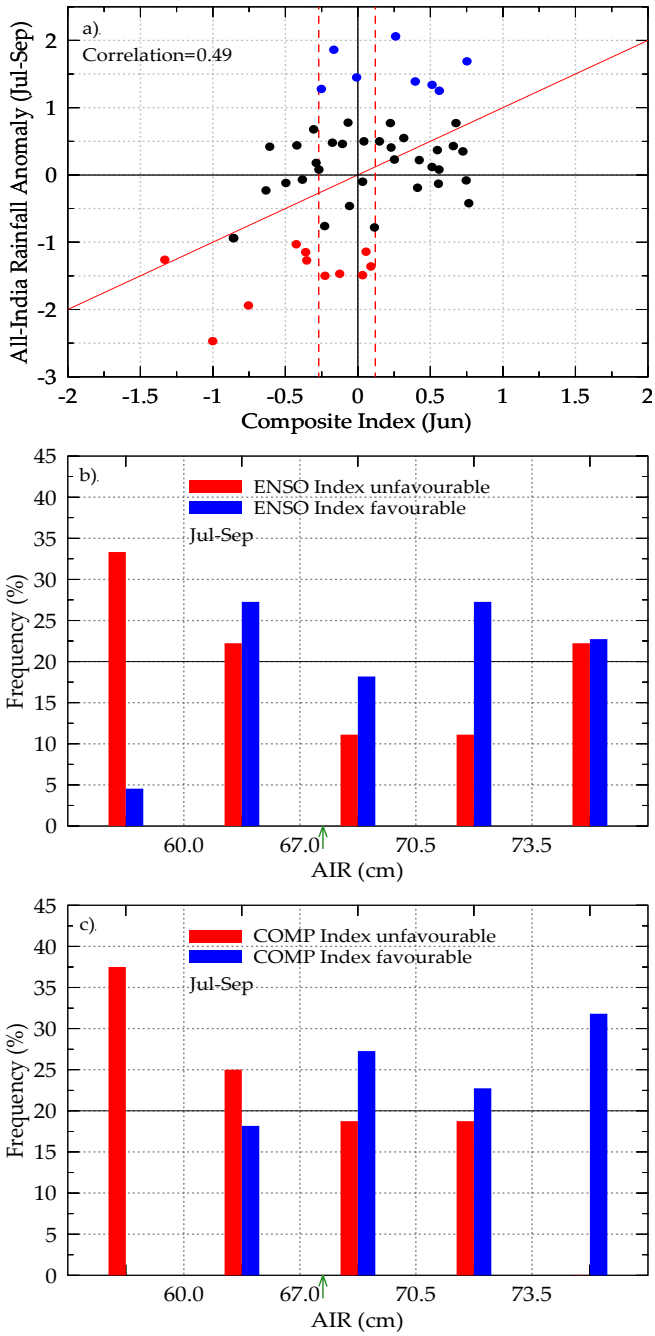

Figure 5.2 a) Normalized all India rainfall anomaly predicted for July-September rainfall against the composite index for June (a); Frequency of occurrence (%) in different categories of normalized July-September anomalies for years for favourable and unfavourable values of ENSO index (b); and of the composite index (c). The green arrows in the x-axes in (b) and (c) indicate the climatological mean July-September all-India rainfall (AIR).

We formed composite indices to predict ISMR, the all-India rainfall during July-September and August-September, by using ENSO and EQUINOO indices for the month proceeding the period for which the rainfall is predicted. For example, all-India rainfall for periods July-September and August-September are predicted using the values of EQWIN and ENSO index prior to that period. The July-September rainfall is significantly correlated with the ENSO index and EQWIN for the month of June and for the linear combination of these two indices determined by bivariate analysis i.e. the composite index. The August-September rainfall is even better correlated with July value of the composite index. In each case, the correlation of the rainfall with the composite index is much higher (statistically significant at 90% level) than that from ENSO index alone. The variation of relationship of the August-September (July-September) rainfall with the composite index for the July (June) determined by multiple linear regression is shown in Figure 5.1a (Figure 5.2a). ENSO and EQWIN together explain 24% and 37% of the variance of the July-September and August-September respectively. Further, it is possible to generate one-sided predictions for the non-occurrence of extremes and low probability of a particular sign of the rainfall anomaly for a certain range of values of the composite index. Thus, it is seen from Figure 1a that if the value of the June composite index is larger than 0.2 (smaller than -0.3), the chance of the July-September rainfall being deficit (in excess) is small and there are no droughts (excess rainfall seasons). When the July composite index (Figure 5.2a) is larger than 0.12 (smaller than -0.12), there are very few years with below (above) normal rainfall and no droughts (excess rainfall seasons).

The frequency distributions in five categories of August-September (July-September) rainfall which have 20% chance when the entire data set is considered for favourable and unfavourable phases of ENSO and of the composite index of the ENSO index and EQWIN, derived by linear multiple regression analysis, for July (June), are shown in Figure 5.1b, c (Figure 5.2b,c) respectively. It is seen that the sign of ENSO has a large impact on the chance of occurrence of the lowest rainfall category in both the cases. It is interesting that ENSO has very little impact on the frequency of the highest July-September rainfall category. On the other hand, EQUINOO and hence the composite index has a substantial impact on the highest July-September rainfall category. Note that for both the cases, unfavourable (favourable) values of the composite index (of magnitude larger than 0.15), there is no chance of occurrence of the highest (lowest) rainfall categories. Thus the incorporation of EQWIN is seen to have had a substantial impact on the frequency distributions.

Sajani Surendran, Sulochana Gadgil (*Indian Institute of Science)*
***Francis P A** (Indian National Centre for Ocean Information Services)*
***and Rajeevan M** (Ministry of Earth Sciences)*

5.2 NCEP CFSv2 retrospective runs and prediction of 2016 Indian Summer Monsoon

Predominantly agrarian economy of India owes greatly to timely monsoon and is therefore imperative to accurately forecast monsoon variability for the benefit of India's economy. Coupling of ocean and atmosphere is found to be necessary to obtain a realistic prediction of tropical climate on various timescales. A fully coupled ocean-land-atmosphere model developed by National Center for Environmental Prediction Climate Forecast System version 2.0 (NCEP CFSv2) was implemented at our institute and seasonal predictions in hindcast mode, initiated with five different initial conditions; 21st April, 26th April, 1st May, 6th May and 11th May, for a period of 38 years starting from 1979, were carried out (Figure 5.3).

Figure 5.3 Setup of retrospective seasonal runs of NCEP CFSv2 made at CSIR-4PI

The model is found to have good skill in simulating rainfall over east and west coast India, although a dry bias exists over land. A correct representation of deep convection processes and sea surface temperature is necessary for simulating the right rainfall over the subcontinent. We have analyzed major characteristics of Indian summer monsoon

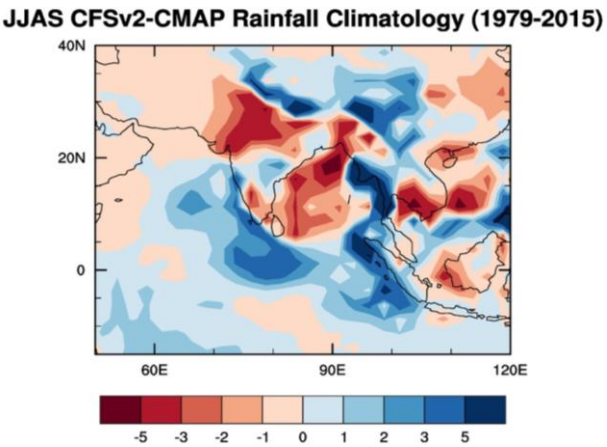

Figure 5.4 Difference between simulated (CFSv2) and observed (CMAP) climatological June to September mean rainfall over 1979-2015 in mm day^{-1}

(JJAS rainfall) by these simulations. The model bias in CFS is first analyzed. The model simulates rainfall maxima over Western Ghats and Bay of Bengal, however, large dry bias exists over Central India. Figure 5.4 shows the bias in model with respect to observation. A pronounced dry bias is seen over regions including parts of monsoon zone.

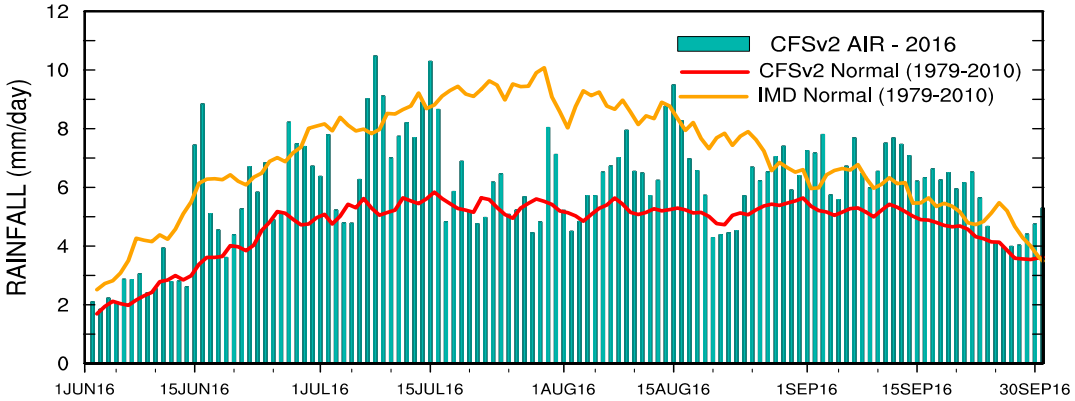

Figure 5.5 Seasonal monsoon forecast for the year 2016 (bars) along with CFSv2 normal (red) and IMD normal (yellow)

CFSv2 forecast for the year 2016 shows above normal rainfall for the country as a whole for the current monsoon season (Figure 5.5).

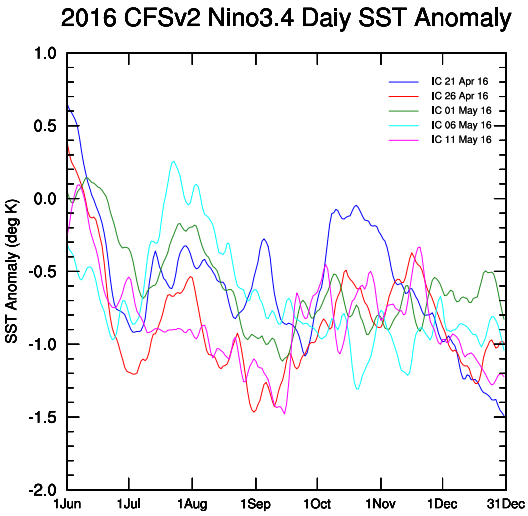

Figure 5.6 Nino 3.4 daily SST anomaly for the monsoon season 2016.

According to the India Meteorological Department (IMD)'s latest update on this year's monsoon, the departure is -3% from long period average for the months June, July and August. Qualitatively there is an agreement between the observation and forecast.

The NINO3.4 sea surface temperature (SST) daily anomaly shows a ENSO neutral conditions in the initial phase of monsoon season that turn to weak La Nina condition in the latter part of the season. (Figure 5.6). This is in good agreement with other observed anomalies.

We are also looking into the teleconnections in CFSv2 to see how well they are captured in the model. From our prior findings, we found higher resolution and deep convection are capable of simulating Indian monsoon with greater fidelity. With this understanding, it is pertinent to look into improving the forecast model for Indian region by removing the model bias.

Rajendran K, Sajani Surendran and Stella Jes Varghese

5.3 Precipitation-aerosol relationship over the Indian region during drought and excess summer monsoon years

The climate effects of aerosols and climatological response of Indian summer monsoon circulation to the direct radiative effect of natural and anthropogenic aerosols is investigated using the Community Atmosphere Model (CAM3) that has comprehensive treatment of the aerosol-radiation interaction, coupled to two different ocean boundary conditions: (1) prescribed climatological sea surface temperatures (SSTs) and (2) an ocean model (CCSM3).As atmospheric general circulation models (GCMs) cannot simulate aerosol loadings directly, this GCM employs a chemical transport model driven by meteorological analysis fields to simulate different species of aerosols. The aerosol climatologies were derived from the simulations of the aerosol transport model.

Our analysis of a suite of climate simulations of a global atmospheric general circulation model (AGCM); the first without any aerosol forcing (henceforth referred to as the AGCM control or `NO_AERO' simulation) and with 5 different representations of aerosol direct radiative forcing, viz., i) total aerosols (10 species of sulphate, carbonaceous, dust and sea salt) referred to as `ALL_AERO', ii) scattering sulphate aerosols alone, `SUL_AERO' and iii) black carbon (soot) alone, `ABS_AERO'. In addition, we have carried out a simulation where the aerosols over the Indian region are prescribed from ISRO's ACE aerosol observations (`ACE_AERO') and a simulation with constant global aerosol simulation, `BKG_AERO'. All the integrations are of 10-year duration after spin-up. Aerosol direct impact due to total aerosols which are dominated by scattering aerosols (as by sulphate aerosols), causes significant reduction in summer monsoon precipitation over India.

Additionally, we have performed climate simulations of the coupled version of the GCM (CGCM, in which CAM3 is coupled to an active ocean model) with total aerosols (`CNTL') and with doubled anthropogenic absorbing aerosols such as black carbon and dust (`DABS_AERO'). These integrations were of 25-year duration after spin-up.

We studied the changes in wind and associated circulation parameters' climatology under different aerosol scenarios (with respect to the control simulation without aerosols (CNTL or NO_AERO)) by analyzing a set of climate simulations with mainly three types of aerosol direct radiative forcing viz. due to (i) total aerosols (AGCM ALL_AERO run), (ii) scattering aerosols (AGCM SUL_AERO run) and (iii) doubled amount of anthropogenic absorbing aerosols (CGCM DABS_AERO run).

Analysis of simulation with doubled anthropogenic aerosols suggests that anthropogenic and natural aerosols significantly affect the circulation but in nearly opposite ways; anthropogenic aerosols tend to have a net local warming effect and strengthening of rainfall and the circulation, but natural aerosols (scattering aerosols) tend to result in net cooling and weakening of cross equatorial monsoon circulation and rainfall.

Aerosol forcing reduces surface solar absorption over the primary convective region of India and reduces the surface and lower tropospheric temperatures. Concurrent warming of the lower atmosphere over the warm oceanic region in the south reduces the land-ocean temperature contrast and thereby weakens the monsoon overturning circulation and the advection of moisture into the landmass. This increases atmospheric convective stability, decreases convection, clouds, precipitation, and associated latent heat release. Our analysis reveals a defining negative moisture-advection feedback that acts as an internal damping mechanism spinning down the regional hydrological cycle and leading to significant circulation changes in response to external radiative forcing perturbations of both scattering aerosols and total aerosols (mixture of scattering and absorbing aerosols).

When total aerosol loading (both absorbing and scattering aerosols) is prescribed, though dust and black carbon aerosols are found to cause significant atmospheric heating over the monsoon region, the aerosol-induced weakening of meridional lower tropospheric temperature gradient (leading to weaker summer monsoon rainfall) more than offsets the atmospheric heating effect of absorbing aerosols, leading to a net decrease of circulation and summer monsoon rainfall. Analysis of simulation with doubled anthropogenic aerosols suggests that anthropogenic and natural aerosols significantly affect the circulation but in nearly opposite ways; anthropogenic aerosols tend to have a net local warming effect and strengthening of the circulation and natural aerosols tend to result in net cooling and weakening of cross equatorial monsoon circulation.

Aerosol radiative forcing perturbation over Indian region alone is found to have both local and remote climate impacts. Analysis of simulation with observed climatological aerosol optical depths (ACE_AERO) shows that marked climate sensitivity occurs not only over the region of loading but over remote tropical regions as well. This suggests the degree of impact of regional aerosols on climate through circulation changes and warrants the need to prescribe realistic aerosol properties in strategic regions such as India.

The degree to which the aerosol impacts the radiative forcing depends on many factors including non-aerosol properties, e.g., presence of cloud and surface albedo. Aerosol forcing is also influenced notably by the surface albedo and cloudiness where it is highly impacted by the clouds which affect the aerosol direct radiative forcing at the TOA level. For example, studies of aerosol simulations show that changes in cloud amount associated with changes in rainfall can strongly limit temperature changes. The aerosol forcing, which includes reflection and absorption, is considerably augmented by the internal climate feedbacks to result in a much more complex spatial distribution than the forcing associated with greenhouse gases which is relatively uniform in space. With all different ways of prescribing aerosols, the simulations tend to reduce the total cloud amount over the continental convective regions. The region with maximum reduction in cloudiness (e.g., north of ~17°N) experiences increased surface solar absorption associated with weakened atmospheric solar depletion due to reduced cloudiness. This suggests that the aerosol-climate direct effect itself is highly non-linear because of aerosols feedback into cloud-radiation interaction, particularly over continental monsoon regions.

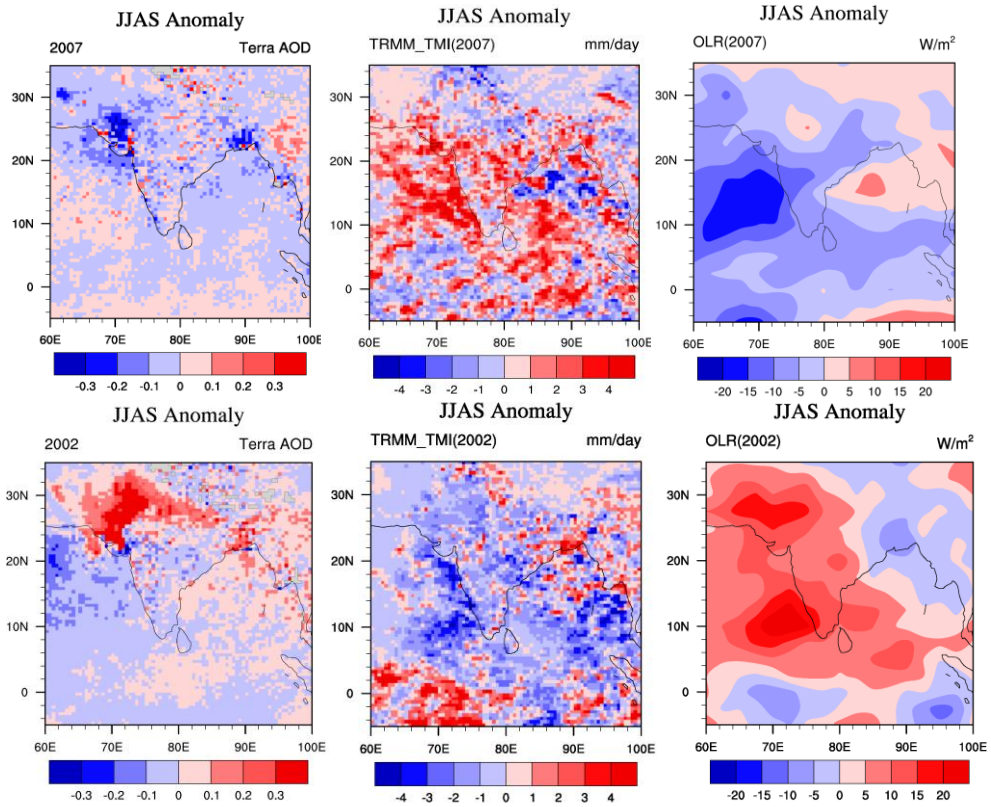

Figure 5.7 Seasonal (JJAS) anomalies of AOD, rainfall and OLR in a drought (top) and excess rainfall year (bottom).

Aerosol Optical Depth (AOD) at 550nm based on Level-2 data from MODIS (MODerate Resolution Imaging Spectroradiometer) remote sensor on-board Terra satellite (Collection 6) gridded to uniform grid is analyzed. In addition, level-3 MODIS cloud effective radius (CER) and cloud optical thickness (COT) since 2000, are also used. For the present analysis we have utilized Tropical Rainfall Measuring Mission (TRMM) 3G68 PR 2A25 and TMI 2A12 for the period 2000-2014. The daily values are computed from the hourly datasets. In addition, (i) outgoing long wave radiation (OLR) measured by the NOAA satellites, archived at http://www.cdc.noaa.gov as a proxy for tropical convection and (ii) ISMR its updates from Indian Institute of Tropical Meteorology (www.tropmet.in) are also analyzed.

All-India summer monsoon rainfall shows considerable interannual variability. This variability is also governed by cloud-radiative feedbacks. In view of this an attempt has been made to investigate the interannual variability in ISMR and its relationship with aerosol radiative effects over the Indian region in monsoon season (June-September, JJAS) using latest satellite derived aerosol datasets.

The AOD, rainfall and convection during 2002 drought monsoon are compared against those during 2007 (Figure 5.7). AOD varies drastically over the Indian region during both years, but the spatial loading of AOD during the drought year 2002 shows that there is persistence of high positive AOD anomalies. The analysis showed that even on monthly scale this difference is

seen, i.e., high values of aerosol optical depth (AOD) occur during the drought monsoon month of July-2002, compared to July-2007 (not shown). Low rainfall amounts during the droughts are associated with an increase in AOD as compared to that in excess monsoon years. Thus, AOD anomalies appear to show near-inverse relationship with precipitation. AOD anomalies were highly positive in July of the drought years, 2002 and 2004 (when the normalized all-India rainfall anomalies were -4.07 and -1.25 respectively) and they were highly negative in July 2005 (when ISMR anomaly was 1.51). We have seen that aerosol and cloud characteristics exhibit strong association to rainfall variability and variability in cloud effective radius and cloud optical thickness is also found to be consistent with aerosol effect.

Sajani Surendran, Rajendran K and Arya V B

5.4 Climate change projections with high confidence using mulit-physics ensemble simulations

Analysis of present-day climatological rainfall simulations over the Indian region shows that while several CMIP5 simulations compare well with observation, a large group of models simulate less than 2 mm/day over the core monsoon region over the Indian subcontinent. Further, the biases in the mean monsoon simulation are found to be related to those in simulating mean seasonal variation of rainfall over the Asia-Pacific region, in addition to the large bias in simulating mean SSTs over the Indo-Pacific region.

Indian summer monsoon rainfall exhibits large interannual variability, which is significantly related to El Niño and equatorial Indian Ocean Oscillation (EQUINOO). The CMIP5 simulations show deficiency in capturing ISMR's link with both equatorial Pacific and Indian Ocean Indices. The projected changes in ISMR is also linked to the changes in these teleconnections which hampers the confidence in their future projections. In addition, the CMIP5 models show significant biases in simulating the present-day precipitation and sea surface temperature (SST) climatologies. In light of these issues, the level of confidence in the predictions made by these climate models for the Indian monsoon region remains limited which could be largely due to inadequacies in the representation of tropical high-resolution processes and the monsoon.

The model used in this study is the latest Meteorological Research Institute AGCM, MRI-AGCM3.2. The model was run at horizontal resolutions of T_L959 (MRI-AGCM3.2S, the 20-km model) and T_L319 (MRI-AGCM3.2H, the 60-km model). At 20-km resolution the model is run with two cumulus convection schemes that were used for the multi-physics ensemble simulations: prognostic Arakawa–Schubert (AS) cumulus convection scheme and a new cumulus convection scheme referred to as Yoshimura scheme (YS). The YS scheme is derived from Tiedtke scheme, but modified to represent all top-level cumulus plumes by interpolating two convective updrafts with maximum and minimum rates of turbulent entrainment and detrainment. At 60-km resolution the model is run with an addition cumulus convection scheme of Kain–Fritsch (KF) convection scheme. For the present-day climate simulation, these models were integrated in Atmospheric Model Intercomparison Project (AMIP)-type runs with the observed historical SST and sea ice data of HadISST.

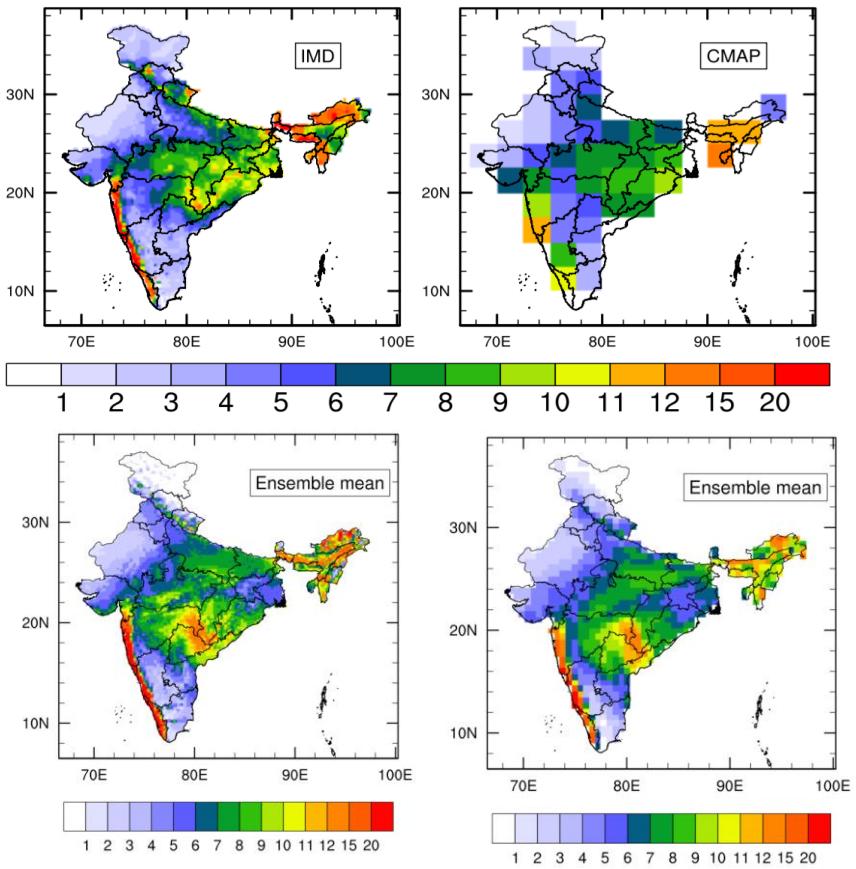

Figure 5.8 JJAS mean rainfall over India (mm day^{-1}) from observations of IMD (top-left) and CMAP (top-right) and MME simulation of present-day mean summer monsoon rainfall at 20-km (bottom-left) and 60-km (bottom-right) resolutions.

These multi physics ensemble runs are used to investigate the future projection of climate change patterns for India. The projections are determined through time-slice integrations of these models, which have shown marked fidelity under different configurations in representing the present-day climate of India in all seasons especially in summer, in simulating all the major features of the mean summer monsoon rainfall over India. For example, the ensemble mean simulation of summer (JJAS) monsoon rainfall over India at 20-km and 60-km resolutions are compared with respective observed climatology based on India Meteorological Department (IMD) data and CMAP rainfall data. The simulations show remarkable skill in capturing the regional rainfall maxima over central India, West-coast orographic region and the northeastern India (Figure 5.8).

The boundary SST data for the future were prepared by superposing: (1) future change in SST projected by CMIP5 multi-model ensemble (MME) mean; (2) the linear trend of SST projected by MME during 2075–2099; and (3) the detrended observed SST for the period 1979–2003. Future sea-ice distribution was obtained in a similar fashion. At 60-km resolution, we have used the projections with four different spatial patterns in sea surface temperature (SST) changes: one with the mean SST changes by the 28 models of the Coupled Model Inter comparison Project Phase 5 (CMIP5) under the Representative Concentration Pathways (RCP)-8.5

scenario, and the other three obtained from a cluster analysis, in which tropical SST anomalies derived from the 28 CMIP5 models were grouped.

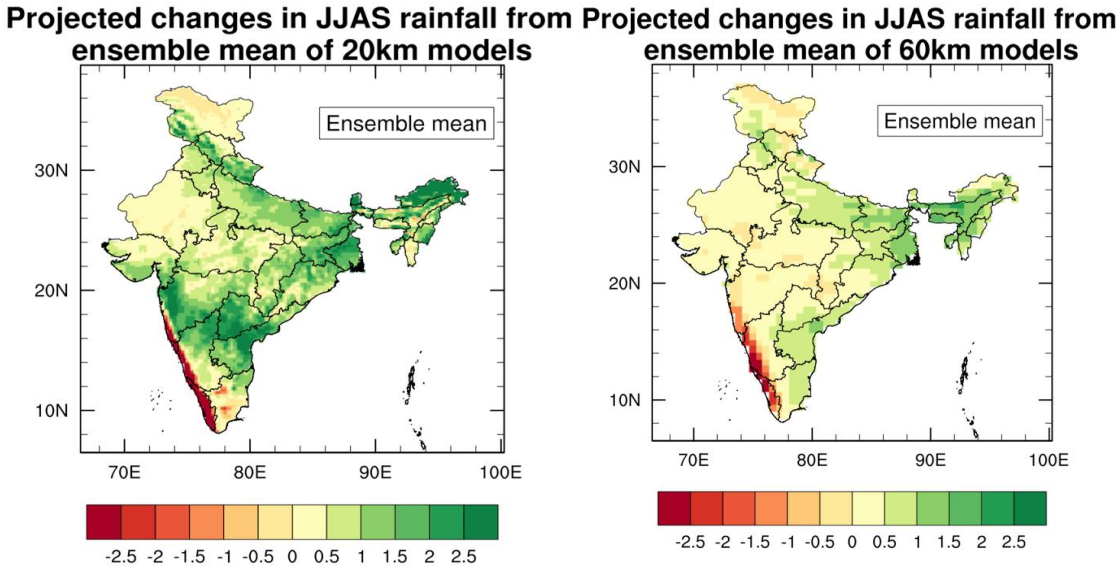

Figure 5.9 Projected future changes in JJAS mean rainfall over India (mm day^{-1}) by MME simulation at 20-km (left) and 60-km (right) resolutions.

Future projections by the MME of time-slice simulations at 20-km and 60-km resolutions under RCP8.5 global warming scenario show widespread but spatially varying increase in rainfall over the interior regions of peninsular, west central, central northeast and northeast India (Figure 5.9) and significant reduction in orographic rainfall over the west coast (consistent with the recent observed trends). Future projections of ISMR with high-resolution regional climate models or IPCC models project relatively uniform change in monsoon rainfall over India. Spatial distribution of the changes summer monsoon precipitation due to global warming shows larger spatial variability with more regional details in simulations with 20-km/60-km resolution (Figure 5.9). This shows that high- resolution simulations are essential to extract useful regional climate change information. The pattern in precipitation is uneven in ultra-high resolution models with distinct spatial heterogeneity.

Over Western Ghats, the drastic reduction of wind by steep orography predominates over the moisture build-up effect (that causes enhanced rainfall under a warmer environment), in reducing the rainfall over the southern west coast. Over this region, faster rate of increase of temperature at higher levels as compared to lower levels (upper-tropospheric warming effect) leads to increased dry static energy and vertical gross moist static stability which in turn weakens the vertical ascent, large-scale monsoon circulation and thereby rainfall.

Rajendran K, Sajani Surendran, Stella Jes Varghese and Kitoh A *(University of Tsukuba)*

5.5 Ultra-high resolution regional climate simulation for Lakshadweep Islands, through dynamical downscaling

The regional climate model simulation with very high resolution is necessary to represent Islands of few kilometer square areas. After several sensitivity studies, we have implemented a very high-resolution non-hydrostatic regional climate model (Weather Research and Forecasting (WRF) model) nested with global model. This dynamical downscaling framework is used to study the regional simulation of a Lakshadweep Island (indicated in the Figure 5.10).

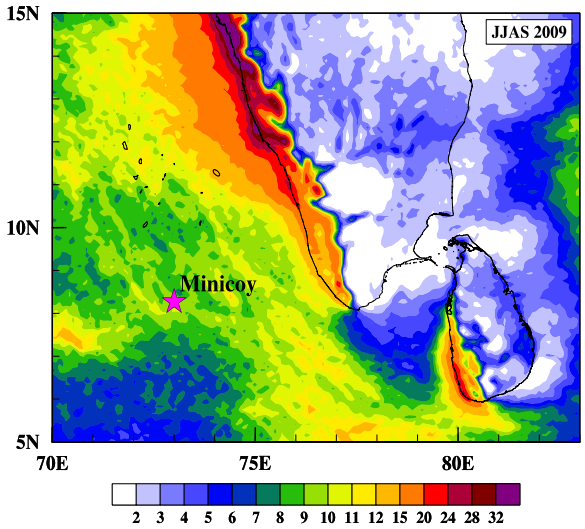

Figure 5.10 Regional model simulated June to September averaged rainfall (mm/day) over the southern part of Indian peninsula. Minicoy station is marked as star.

In order to test the skill in simulating present-day climate, we have performed a 12-month simulation of the year 2009 with 3 domains and best configuration tailored for Indian region; the model integration is started from 1st January and ends on 31st December. This regional model have high dependency on the lateral boundary forcing (LBF), here the reanalysis data is used as the LBF.

For validating the regional simulation, we have selected Minicoy (8.3°N, 73°E), which is one of the Lakshadweep Islands. The 2-meter temperature (T2M) and precipitation are compared with the 3-km resolution regional simulation for the year 2009. Figure 5.10 shows the model simulated June to September averaged rainfall (mm/day) over the peninsular India and Lakshadweep region, inside of which the Minicoy station is marked as star (Magenta). The simulated precipitation is well comparable with the TRMM observation (not shown). In Figure 5.11, the top panel shows the pentad precipitation from the Minicoy station observation and the bottom panel shows the model-simulated pentad precipitation for the year 2009. The model precipitation of Minicoy is computed based on the average of 4-grid point around the station location (8.3°N, 73°E). Despite a subtle tendency for the simulated to overestimate precipitation in some pentad, the simulation is well comparable with the

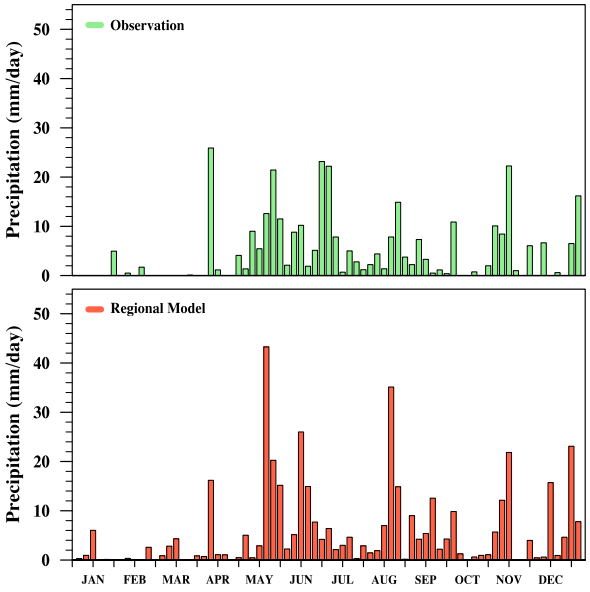

Figure 5.11 Pentad precipitation (mm/day) for the year 2009, from Minicoy Island station observation (top) and regional model simulation (bottom)

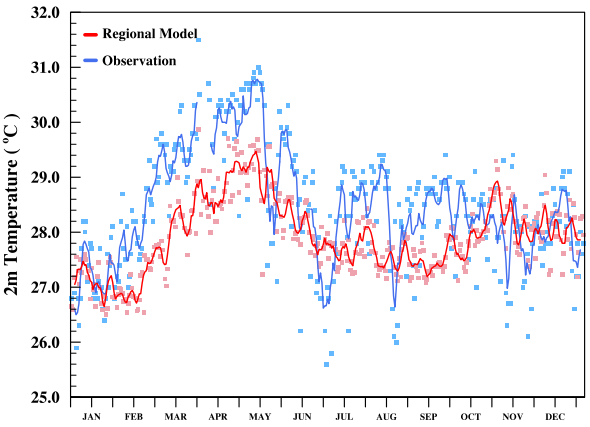

Figure 5.12 Daily 2-meter temperature (°C) for the year 2009, from Minicoy Island station observation (Blue) and regional model simulation (Red)

observation. The model simulated T2M of the island shows closer match with the observation (Figure 5.12). From February to May, the magnitude of simulated T2M is slightly underestimated and afterwards the simulation and observation follow closely. Hence, these results indicate that the model has reasonable fidelity in simulating the regional climate information at shorter time scales.

Similarly, longer period simulation needed to be analyzed to understand the model reliability in simulating the regional climate, which reveals numerous regional details and also this model can be employed for simulating the future projections. And we can extract many climate related variables from this very high-resolution regional climate model to find the changes in the climate and extremes. This is very useful for assessing potential impact of climate change of the respective region and is crucial for agriculture and economy as well as it helps to plan and execute the adaptability.

Jayasankar C B and Rajendran K

5.6 Diagnostic study of NCEP CFSv2 retrospective runs performed at CSIR-4PI

The vagaries of monsoon are complex; the climate modeling community considers it as challenging to understand and predict its behavior. Predominantly agrarian economy of India owes greatly to timely and adequate monsoon. Thus it is imperative to forecast monsoon to serve this purpose. Climate models are mathematical representation of climate by dividing earth, ocean and atmosphere into a grid. Coupling of ocean and atmosphere is advisable to obtain a realistic simulation of monsoon on various timescales.

As part of National Monsoon Mission of India, a fully coupled ocean-land-atmosphere model, National Centers for Environmental Prediction (NCEP) Climate Forecast System Version 2.0 (CFSv2) was installed and tested at the HPC in CSIR-4PI, Bangalore. The atmospheric component of the model is NCEP Global Forecast System (GFS) model with triangular truncation of 126 or 382 waves in horizontal and finite differencing in the vertical with 64 sigma-pressure hybrid layers. It is coupled to a four-layer NOAH Land Surface Model and two-layer Sea Ice Model. The oceanic component is Modular Ocean Model version 4 (MOM4).

The model is integrated with five different initial conditions; 21st April, 26th April, 01st May, 06th May and 11th May and this 5-member ensemble runs are analyzed for Indian summer monsoon (June to September) season.

Figure 5.13 shows the JJAS climatology of the five ensemble members along with corresponding observed climatology based on GPCP data for the period 1979-2016.The climatology shows remarkable skill in simulating the spatial distribution of rainfall over India, although there is dry bias prevalent over land.

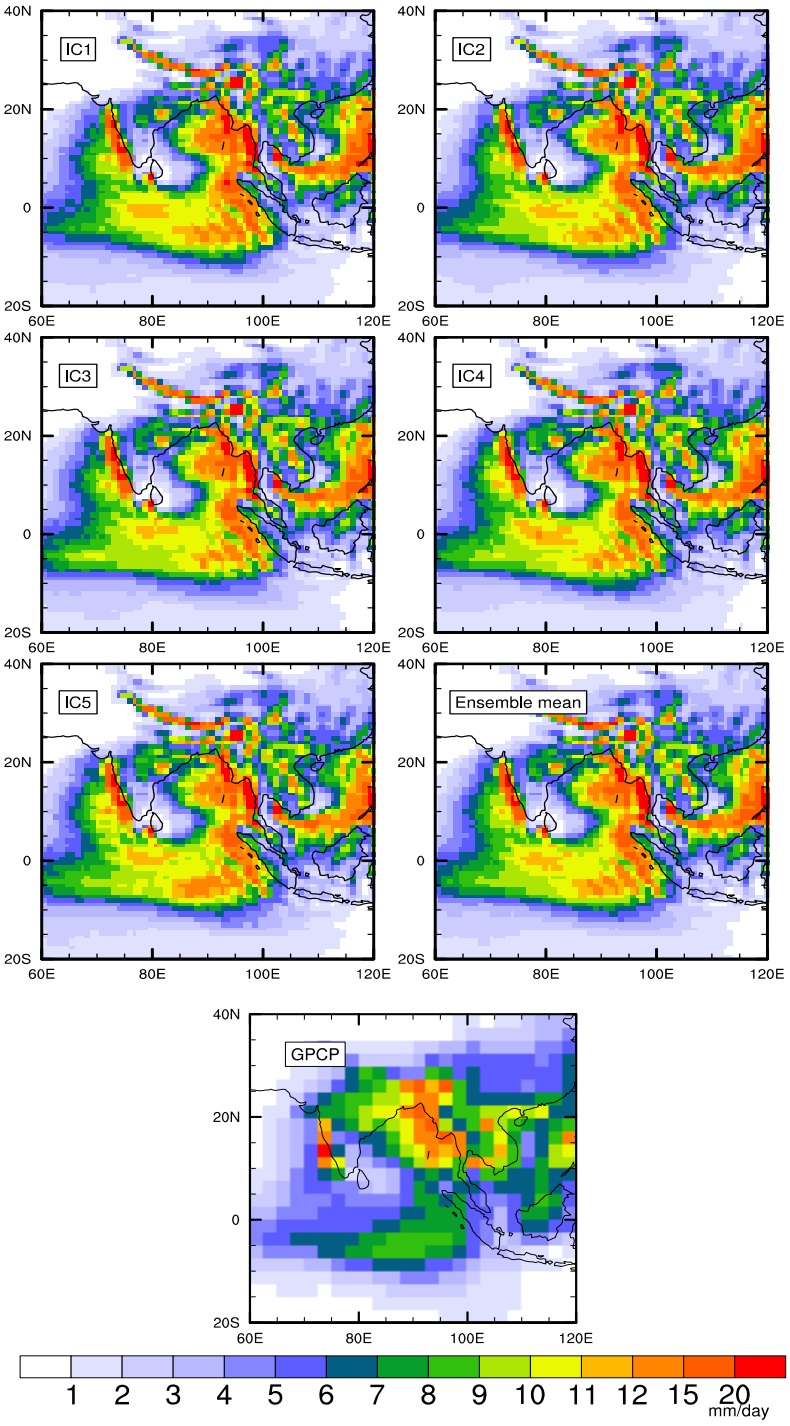

Figure 5.13 JJAS rainfall climatology for various initial conditions (IC1: 21st April, IC2: 26th April, IC3: 1st May, IC4: 6th May, IC5: 11th May), ensemble mean and observation (TRMM 3B43) for the period 1979-2015.

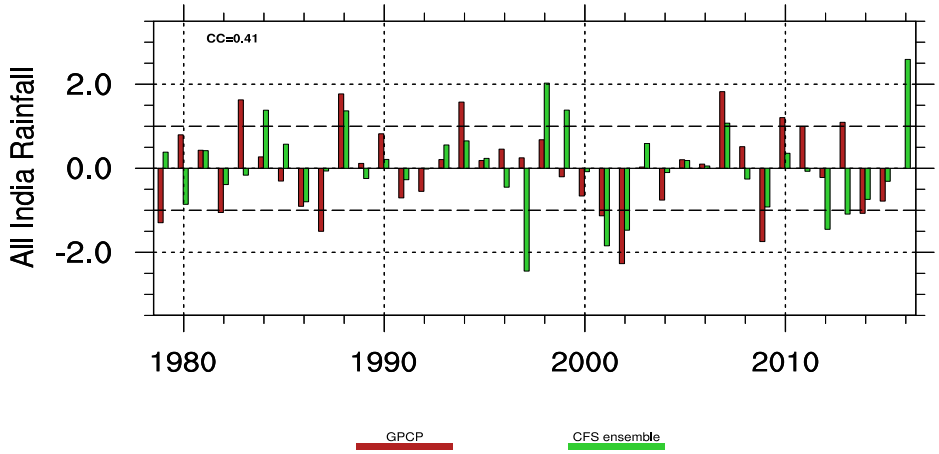

Figure 5.14 Interannual variability (IAV) of all-India summer monsoon rainfall (ISMR) during 1979-2016 in ensemble mean of NCEP CFSv2 retrospective runs and GPCP observed rainfall.

The interannual variability of the model simulation helps in understanding how well it can capture the summer monsoon variability and its teleconnections with El Niño-Southern Oscillation (ENSO), Equatorial Indian Ocean Oscillation (EQUINOO) etc. The standardized anomaly of all India averaged rainfall of the model is compared with that of observation (GPCP) for the period 1979-2016. Figure 5.14 shows the interannual variability of Indian summer monsoon rainfall. The data shows a correlation coefficient of 0.41 which is a measure of the fidelity of the model in simulating the interannual variability. Thus, it is seen that there exists a lot of scope for improving the skill of seasonal prediction of the model.

Stella Jes Varghese, Sajani Surendran and Rajendran K

5.7 Aerosol-Cloud relationship and aerosol indirect effect on clouds

Aerosols are tiny floating particles (liquid or solid) in the atmosphere. These particles alter earth radiation budget by scattering and absorbing the solar radiation that energize the formation of clouds. Our study investigates the aerosol-precipitation interactions over Indian region during contrasting monsoon years. In order to understand the aerosol-precipitation relationship the knowledge of the interaction between aerosols-clouds are inevitable.

To monitor atmospheric aerosols, the best possible method is through satellite measurement, because the ground-based measurements (Lidar and Sun photometer) and in-situ measurements (aircraft and balloons) are very limited in space and time and these aerosol particles transport over long distance from the source region.

The present study uses latest version of various satellite derived aerosol product such as MODIS (MODerate Resolution Imaging Spectro-radiometer). The aerosol parameter we analyzed for this study is aerosol optical depth (AOD), which is the measure of how much

aerosol exists in the atmosphere. AOD has been estimated based on 550nm Level-2 (swath data) MODIS data. MODIS atmospheric aerosol product provides full global coverage of aerosol properties from Dark Target and Deep Blue algorithm. The frequency of MODIS Level-2 data is 144 files per day. Each granule is binned and averaged to uniform grid to make daily data at 0.5^0 x 0.5^0 resolution. Cloud properties such as Cloud Effective Radius (CER), Cloud Optical Thickness (COT), Cloud Top Height (CTH) are analyzed using MODIS Level-3 processed data at 1°×1°resolution.

Tropical Rainfall Measuring Mission (TRMM) derived daily and monthly data for the period 2000-2014 is used. Daily and monthly interpolated OLR at 2.5°×2.5°resolution from NOAA satellites is also utilized. In addition, ERA-Interim circulation dataset at 0.5°×0.5°resolution is also used for this study. To analyze the latent heat profile, we used TRMM monthly latent heat product. This data is available from December 1997 to June 2011 at horizontal resolution of 0.5°.

JJAS climatology of AOD shows high values of AOD over the Indo-Gangetic plains (Figure 5.15), where most of the industries are located and are densely populated. During monsoon period low-level winds are stronger and transports marine aerosols into the land region. OLR serves as the proxy for the rainfall.

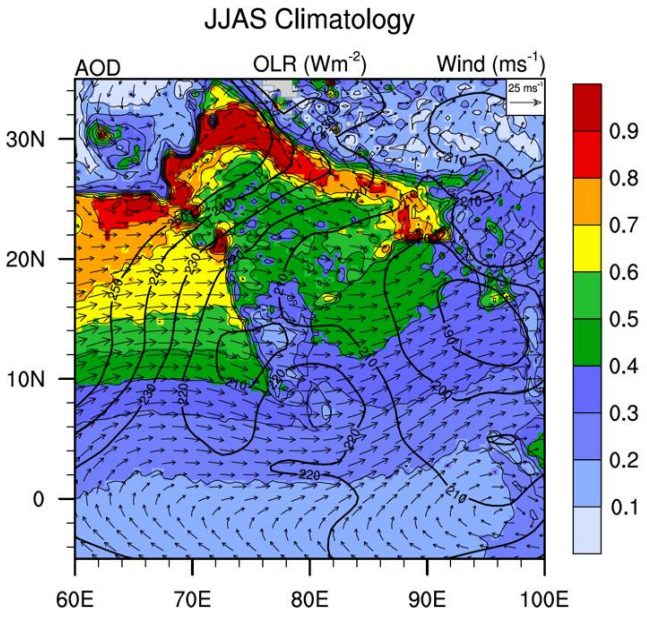

Figure 5.15 JJAS Climatology of AOD, OLR and winds for the period 2000-2014. The shaded contours corresponding to AOD, on which overlaid are winds (arrows) and convection (OLR in contour lines).

Aerosols can interact with clouds and precipitation in many ways, acting either as cloud condensation (CCN) or ice nuclei (IN), or as absorbing particles, redistributing solar energy as thermal energy inside cloud layers. In the context of global climate change, aerosol and cloud interactions remain the most uncertain factor because the mechanisms that link aerosol to cloud properties change are carried out through processes that are not well understood. Investigations involving cloud and aerosol showed positive, negative or no correlation between aerosol and cloud properties in general and cloud water path particularly. It is observed that for AOD value below the peak (AOD_{peak}), mean cloud properties especially the cloud water path (CWP), and mean AOD are positively correlated. The correlation between mean CWP and mean AOD is negative for aerosol loading above AOD_{peak}.

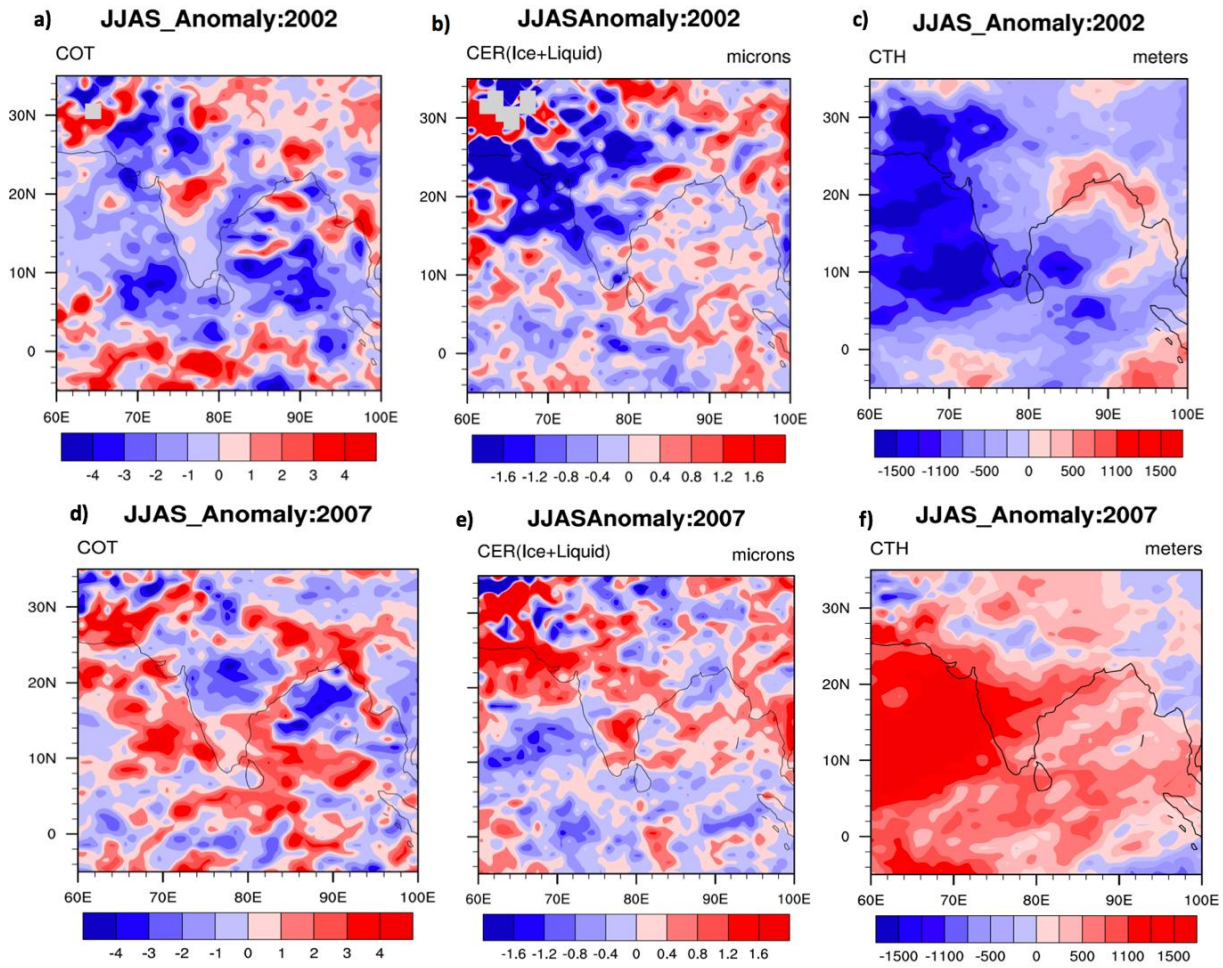

Figure 5.16 JJAS anomalies of cloud properties such as cloud optical thickness (COT), cloud effective radius (CER) and cloud top height (CTH) during 2002 drought year (a-c) and excess monsoon of 2007 (d-f).

The comparison of JJAS anomalies of COT, CER and CTH during drought monsoon 2002 and excess monsoon 2007 is shown in Figure 5.16. As aerosols are effective CCN, their variability is expected to modulate the cloud optical properties such as CER and COT. Overall, anomalies are significantly lower in 2002 while AODs are higher, implying an association between aerosols and clouds, and possibly an evidence for the indirect radiative effect of aerosols on clouds. These results emphasize the fact that when aerosols become abundant, they can decrease the cloud effective radius. COT and CTH are also less. More analysis is being done to understand this aspect.

Arya V B and Sajani Surendran

5.8 Preliminary study of convectively coupled equatorial waves

Convectively Coupled Equatorial Waves (CCEWs) are important class of propagating disturbances which affect tropical mean convection and climate. They produce prominent intraseasonal fluctuations over tropics. Some of them travel all around the world zonally and

some move in pole ward direction from equator. Proper understanding of these waves is essential for the prediction of variability at all the time scales.

Outgoing Long wave Radiation (OLR) measurement is the easiest way to track the convective components of convectively coupled waves. OLR interpreted in a large scale sense acts as a proxy for large areas of cloudiness/convection. In the tropics, a low OLR value represents an active convection whereas a high OLR value represents a suppressed convection. So in this study we are using OLR as a proxy for convection. As an initial step we focus on 30-70 day mode before studying the CCEWs.

Here we use daily interpolated OLR of 2.5^{o} resolution from NOAA. From daily OLR, 30-70 day anomaly was filtered out. It is evident from figures that there are well defined northward propagations of convective anomalies from equator region. We take a wet year (excess rainfall year,1988) and a dry year (deficit rainfall year,1982) to see the contrasting behaviours of intraseasonal oscillations (ISOs).

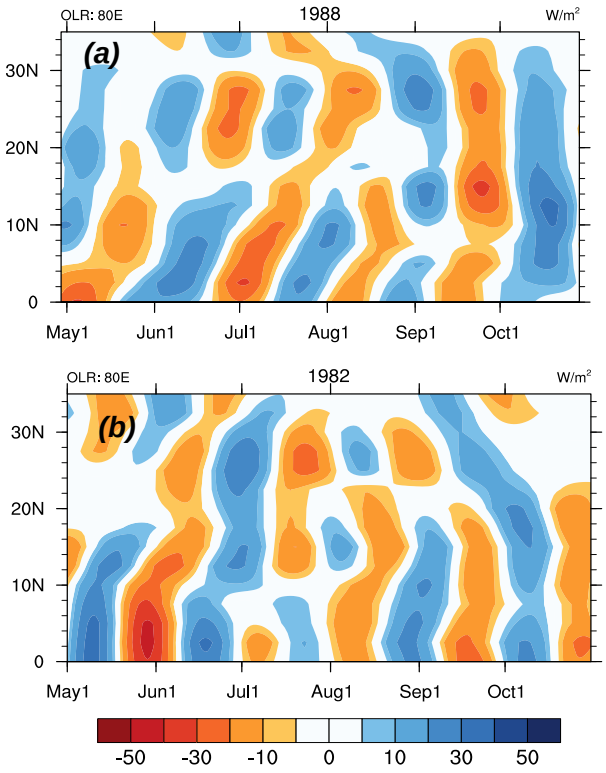

Figure 5.17 30-70 day OLR anomalies at 80^{o}E longitude in a) 1988 and b) 1982.

Figure 5.17 represents 30-70 day filtered OLR anomalies of 1988(an excess monsoon year) and 1982 (a deficit monsoon year) during May to October. Here red contours represent negative anomalies whereas blue contours represent positive anomalies. These coherent bands of positive and negative anomalies represent break and active phases respectively. In 1988, starting from May, a convective phase moves from equator to north and it reaches land by the end of May. This coincides with the monsoon onset. Alternate phases depict the occurrence of near-inverse anomalies between continental India (~15^{o}-30^{o}N) and equatorial region (0^{o}-10^{o}N). In 1988, propagations are clearer, coherent and with longer period compared to 1982 during which the propagations are either fast or incoherent.

Nirmala J Nair, Rajendran K and Sajani Surendran

5.8 An algorithm for TRMM PR spectral latent heating retrieval

Even though Tropical convective precipitation systems have major role in the global climate system, our understanding of it is very poor because of not only its complexity in spatial and vertical distribution but also having very short lifespan for such systems. Diabatic heating estimates used in this study are from TRMM – PR utilizing the Spectral Latent Heat (SLH)

algorithm. TRMM satellite launched in December 1997 is having a space borne precipitation radar, which has a 13.8GHz Ku band frequency. It is having temporal resolution of around 16 orbits per day and horizontal resolution of around 5 km. Its swath width is around 247 km consists 49 angle bins. One granule of PR data is one orbit which is having around 9140 scans. The latent heat profiles have 19 layers at the fixed heights of 0.0-0.5 km, 0.5-1 km, 1-2 km etc. up to 17-18km.

We have taken this Level-2 swath data and converted it into gridded data using nearest neighbor algorithm. Here for distance calculations we used great circle distance formula. The resultant data is having spatial resolution of 0.25 degree and we keep the temporal and vertical resolution same as the original data for not to miss even short life convective systems. Using this data, we analyze the four dimensional distributions (including time) of the apparent heat source (Q_1) – radiative heating (Q_R), apparent moisture sink (Q_2) and Latent heating in relation with the near surface precipitation rate and storm top height. This resultant data set clearly explains the major characteristics of tropical convection.

Also we develop a vertically integrated $Q_1 - Q_R$, Q_2 and Latent Heat utilizing a new algorithm build on a time based RMS weighting function. Figure 5.18 is the monthly average of weighted vertical Integrating $Q_1 - Q_R$ for the month of July 2003. Here we have taken daily average of the gridded data and then for each spatial grid we have computed a RMS value based on 31 days of July and by taking this RMS value as weighting function for estimating the daily vertical Integration. The pattern explains the major features of tropical convection such as ITCZ distribution including Indian summer monsoon convective centres.

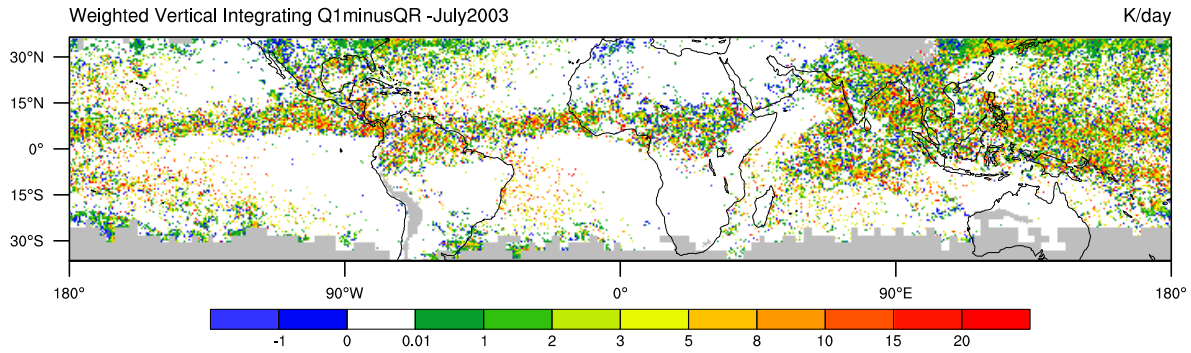

Figure 5.18 is the monthly average of weighted vertical Integrating $Q_1 - Q_R$ for the month of July 2003

This compares well with the monthly averaged near surface precipitation rate for the same month. From this distribution we could explain the tropical precipitating cloud systems. So in future we plan to apply these techniques for all the remaining data set so that we could analyze the tropical convection structure and explain its generic aspects.

Athira U Nambeesan, Rajendran K and Sajani Surendran